

# Surface Modification of Graphene Nanosheets with Gold Nanoparticles: The Role of Oxygen Moieties at Graphene Surface on Gold Nucleation and Growth

Gil Goncalves,<sup>†</sup> Paula A. A. P. Marques,<sup>\*,†</sup> Carlos M. Granadeiro,<sup>‡</sup> Helena I. S. Nogueira,<sup>‡</sup> M. K. Singh,<sup>†</sup> and J. Grácio<sup>†</sup>

<sup>†</sup>TEMA–NRD, Mechanical Engineering Department, University of Aveiro, 3810-193 Aveiro, Portugal, and  
<sup>‡</sup>CICECO, Department of Chemistry, University of Aveiro, 3810-193 Aveiro, Portugal

Received April 16, 2009. Revised Manuscript Received September 3, 2009

Graphene sheets, which possess unique nanostructure and a variety of fascinating properties, are considered as promising nanoscale building blocks of new nanocomposites, namely as a support material for the dispersion of metal nanoparticles. One of the methodologies used to prepare graphene sheets is the chemical exfoliation of graphite in aqueous medium, which produces oxygen functionalized graphene sheets. Here, we show that the presence of oxygen functionalities at the graphene surface provides reactive sites for the nucleation and growth of gold nanoparticles. Gold nanoparticles are effectively grown at functionalized graphene surfaces using a simple chemical method in aqueous medium. The nucleation and growth mechanism depends on the degree of oxygen functionalization at the graphene surface sheets, no gold nanoparticles are obtained at totally reduced graphene surfaces. Additionally, our studies indicate that the graphene/gold nanocomposites are potential substrates for SERS (surface enhanced Raman scattering) in particular for single gold nanoparticle SERS studies.

## 1. Introduction

Graphene is one of the most exciting materials being investigated today, not only out of academic curiosity but also with potential applications in mind. Graphene, by definition, is a single-layer, two-dimensional material, but graphene samples with two or more but less than ten layers are equally interesting.<sup>1</sup> Most of the physical studies of graphene have been carried out on single-layer sheets obtained by micromechanical cleavage techniques, but the preparation of large quantities of different types of graphene and their characterization is currently the focus of much interest.<sup>2–4</sup> Graphene can be obtained by exfoliation of graphite that results in well separated 2D aromatic sheets composed by sp<sup>2</sup>-bonded carbon atoms.<sup>5</sup> Graphene sheets offer extraordinary electronic, thermal, and mechanical properties and are expected to find a variety of applications, such as sensors, nanocomposites, batteries, supercapacitors, and hydrogen storage.<sup>6</sup>

Recently, a large number of papers have described the dispersion and exfoliation of graphene oxide (GO).<sup>7–9</sup> This material consists of graphene like sheets, chemically functionalized with oxygen groups such as hydroxyls and epoxides that stabilize the dispersion of the nanosheets in water.<sup>10</sup> With a thermal treatment (deoxygenation) or a chemical reduction (for example using hydrazine), GO could be reduced to restore the graphene structure and its conductive properties.<sup>5,6,11,12</sup> From the chemical point of view, the presence of oxygen functionalities at GO surface may be very interesting because they provide reactive sites for chemical modification using known carbon surface chemistry. From the literature, it is known that strong interfacial interactions with the surfaces of graphene-containing materials, such as carbon nanotubes, carbon fibers, and highly oriented pyrolytic graphite, require that these materials be chemically functionalized in a manner that permits the formation of a strong bond with the

\*Corresponding author. E-mail: paulam@ua.pt.

- (1) Rao, C. N. R.; Kanishka, B.; Subrahmanyam, K. S.; Govindaraj, A. *J. Mater. Chem.* **2009**, *19*, 2457.
- (2) Tung, V. C.; Allen, M. J.; Yang, Y.; Kaner, R. B. *Nat. Nanotechnol.* **2009**, *4*, 25.
- (3) Afanasov, I. M.; Morozov, V. A.; Kepman, A. V.; Ionov, S. G.; Seleznev, A. N.; Van Tendeloo, G.; Audeev, V. V. *Carbon* **2009**, *47*, 263.
- (4) Biswas, S.; Drzal, L. T. *Nano Lett.* **2009**, *9*, 167.
- (5) Jang, B. Z.; Zhamu, A. *J. Mater. Sci.* **2008**, *43*, 5092.
- (6) Li, D.; Muller, M. B.; Gilje, S.; Kaner, R. B.; Wallace, G. G. *Nat Nanotechnol* **2008**, *3*, 101.
- (7) Steurer, P.; Wissert, R.; Thomann, R.; Mulhaupt, R. *Macromol. Rapid Commun.* **2009**, *30*, 316.

- (8) Yang, D.; Velamakanninb, A.; Bozoklu, G.; Park, S.; Stoller, M.; Piner, R. D.; Stankovich, S.; Jung, I.; Field, D. A.; Ventrice, C. A.; Ruoff, R. S. *Carbon* **2009**, *47*, 145.
- (9) Wang, G. X.; Wang, B.; Park, J.; Yang, J.; Shen, X. P.; Yao, J. *Carbon* **2009**, *47*, 68.
- (10) Hernandez, Y.; Nicolosi, V.; Lotya, M.; Blighe, F. M.; Sun, Z. Y.; De, S.; McGovern, I. T.; Holland, B.; Byrne, M.; Gun'ko, Y. K.; Boland, J. J.; Niraj, P.; Duesberg, G.; Krishnamurthy, S.; Goodhue, R.; Hutchison, J.; Scardaci, V.; Ferrari, A. C.; Coleman, J. N. *Nat. Nanotechnol.* **2008**, *3*, 563.
- (11) Hirata, M.; Gotou, T.; Horiuchi, S.; Fujiwara, M.; Ohba, M. *Carbon* **2004**, *42*, 2929.
- (12) McAllister, M. J.; Li, J. L.; Adamson, D. H.; Schniepp, H. C.; Abdala, A. A.; Liu, J.; Herrera-Alonso, M.; Milius, D. L.; CarO, R.; Prud'homme, R. K.; Aksay, I. A. *Chem. Mater.* **2007**, *19*, 4396.

material being deposited.<sup>13,14</sup> In the case of deposited metal nanoparticles used in fuel cells for example, these chemical functionalities usually take the form of covalently bonded oxidized carbon species, such as alcohols (C–OH), carbonyls (C=O, as in aldehydes and ketones), and acids (COOH). Although many chemical techniques exist for their introduction, such as aqueous sonication<sup>15</sup> and plasma techniques,<sup>16</sup> they are most often introduced by strong sulfuric/nitric acid treatment.<sup>17,18</sup> In the case of GO nanosheets that are directly obtained from the chemical exfoliation of graphite, the oxygen chemical functionalities essential for further chemical reactions are already present. Therefore, GO can be considered as promising nanoscale building blocks with ultrahigh surface area to prepare new nanocomposites.

The impact in the association of graphene with metallic nanoparticles producing nanocomposites with promising potential applications such as chemical sensors, energy storage, catalysis, and hydrogen storage, among others has captured the interest of some researchers.<sup>19–21</sup> Another important feature of the adhesion of metal nanoparticles to the graphene is the inhibition of aggregation of the resulting graphene sheets in dry state. By functioning as a spacer, the metal nanoparticles increase the distance between the graphene sheets, thereby making both faces of graphene accessible.<sup>19</sup>

Most of the published papers about the preparation of graphene/metal nanocomposites makes use of organic spacers, like octadecylamine, to anchor the metallic nanoparticles to the graphene surface or organic solvents such as tetrahydrofuran, methanol, and ethylene glycol.<sup>20</sup> In this paper, we present the preparation and characterization of graphene/gold nanocomposites using a simple synthesis method in aqueous medium. Gold was selected for its unique optical and surface properties that attract a great deal of attention because of their potential applications in catalysis, optics, and nanobiotechnology.<sup>22</sup> We show that the presence of the oxygen functionalities at the graphene oxide surface plays an important role on the nucleation and growth of gold nanoparticles. We illustrate this by preparing the gold nanoparticles in the presence of graphene sheets with different degrees of functionalization. We also anticipate the potential application of the prepared graphene/gold nanocomposite as a substrate for surface enhanced Raman scattering (SERS).

## 2. Experimental Section

**Synthesis. Chemical Exfoliation of Graphite.** The chemical exfoliation of graphite was based on the method suggested by Hummers and Offeman.<sup>23</sup> Concentrated H<sub>2</sub>SO<sub>4</sub> (50 mL) was added into a 250 mL flask filled with graphite (2 g) at room temperature. The flask was cooled to 0 °C in an ice bath, followed by slow addition of KMnO<sub>4</sub> (7 g); the flask was then allowed to warm to room temperature. The temperature was then raised to 35 °C with a water bath, and the mixture was stirred with a Teflon-coated magnetic stirring bar for 2 h. Afterward, the reaction mixture was cooled with an ice bath, followed by the addition of distilled water in excess to the mixture. H<sub>2</sub>O<sub>2</sub> (30 wt % in water) was then added until gas evolution ceased.

The resultant suspension was intensively washed, first with a diluted solution of HCl (0.1 mol dm<sup>−3</sup>) and then with distilled water by filtration, and was then centrifuged at 3,000 rpm to remove residual unexfoliated graphite and further oxidant agents.

The resulting material was dried by lyophilization in order to obtain a nonagglomerated powder. This material will be further referred as graphene oxide (GO).

**Thermal Treatment of Graphene Oxide.** Twenty milligrams of the previous prepared GO was inserted into a quartz tube in an argon atmosphere. After that, the tube was placed in a preheated furnace at 1050 °C during 30 s. This treatment is used to promote further exfoliation of the graphene sheets and at the same time reduce the oxygen moieties.<sup>12</sup> Hereafter, this material will be referred as graphene thermally reduced (GTR).

**Reduction of Graphene Oxide with Hydrazine.** GO (100 mg) was loaded in a 250-mL round-bottom flask and water (100 mL) was then added, yielding an inhomogeneous yellow-brown dispersion. This dispersion was sonicated until it became clear with no visible particulate matter. Hydrazine hydrate (1.00 mL, 32.1 mmol) was then added and the solution was heated in an oil bath at 100 °C under a water-cooled condenser for 24 h over which the reduced GO gradually precipitated out as a black solid. This product was isolated by centrifugation and washed copiously with water. The resulting material was then lyophilized. Hereafter, this material will be referred as GHR.

**Synthesis of Graphene/Au Nanocomposites.** The synthesis of graphene/Au nanocomposites was based on the reduction of gold(III) complex by sodium citrate.<sup>24</sup> Typically, 2.5 mL of a graphene aqueous suspension (1.5 mg/mL) was added to 50 mL of HAuCl<sub>4</sub> solution (0.24 mmol dm<sup>−3</sup>). The resultant suspension was aged during 30 min to promote the interaction of gold ions with the graphene surface. After that, the solution was heated until 80 °C, after which 940 μL of sodium citrate (0.085 mol dm<sup>−3</sup>) was added dropwise. The reaction was kept at these conditions during 1 h.

The resultant nanocomposite was washed with distilled water using centrifugation (3000 rpm) to remove the free gold nanoparticles that formed in solution. The final nanocomposite was dried by lyophilization.

This process was repeated for the three different types of graphene: GO, GTR, and GHR.

**Preparation of Samples for SERS.** First, a few drops of the graphene/gold nanocomposites aqueous suspensions were deposited in silica substrates and dried in a desiccator over silica gel. A drop of an ethanolic solution of rhodamine 6G (0.1 mol dm<sup>−3</sup>)

- (13) Zhang, G.; Sun, S.; Yang, D.; Dodelet, J. P.; Sacher, E. *Carbon* **2008**, *46*, 196.
- (14) Liang, C.; Xia, W.; Soltani-Ahmadi, H.; Schluter, O.; Fischer, A.; Muhler, M. *Chem Commun* **2005**, 282.
- (15) Yang, D. Q.; Rochete, J. F.; Sacher, E. *J. Phys. Chem. B* **2005**, *109*, 7788.
- (16) Tseng, C. H.; Wang, C. C.; Cheng, C. Y. *Chem. Mater.* **2007**, *19*, 308.
- (17) Li, L.; Wu, G.; Xu, B. Q. *Carbon* **2006**, *44*, 2973.
- (18) Zhang, G.; Sun, S.; Yang, D.; Dodelet, J. P.; Sacher, E. *Carbon* **2008**, *46*, 196.
- (19) Si, Y. C.; Samulski, E. T. *Chem. Mater.* **2008**, *20*, 6792.
- (20) Muszynski, R.; Seger, B.; Kamat, P. V. *J. Phys. Chem. C* **2008**, *112*, 5263.
- (21) Xu, C.; Wang, X.; Zhu, J. W. *J. Phys. Chem. C* **2008**, *112*, 19841.
- (22) Shen, C. M.; Hui, C.; Yang, T. Z.; Xiao, C. W.; Tian, J. F.; Bao, L. H.; S. T. Chen, S. T.; Ding, H.; Gao, H. J. *Chem. Mater.* **2008**, *20*, 6939.

- (23) Hummers, W. S.; Offeman, R. E. *J. Am. Chem. Soc.* **1958**, *80*, 1339.
- (24) Lee, P. C.; Meisel, D. *J. Phys. Chem.* **1982**, *86*, 3391.

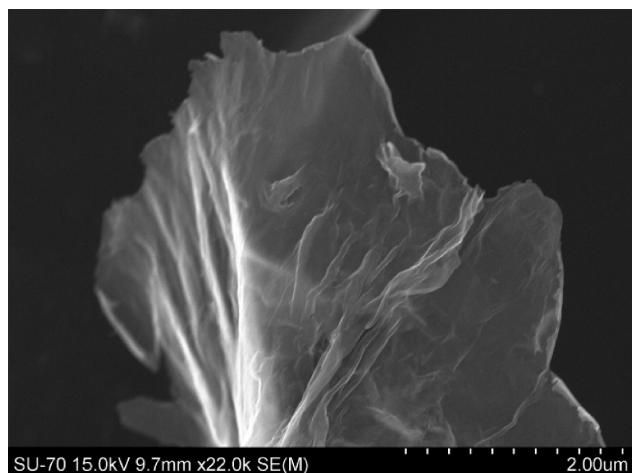


**Figure 1.** Representative SEM micrograph of graphene oxide sheet.

was then deposited onto the surface of the dried nanocomposites. After the ethanol evaporation, the Raman spectrum of the sample was registered directly.

**Characterization.** Scanning electron microscopy (SEM) images were obtained using a FEG-SEM Hitachi S4100 microscope operating at 25 kV. Transmission electron microscopy (TEM) was performed using a Hitachi H-9000 operating at 300 kV. The samples for TEM were prepared by depositing an aliquot of the graphene suspension onto a carbon-coated copper grid and then letting the solvent evaporate.

The FTIR spectra of different samples of graphene were recorded from KBr pellets (Aldrich, 99%, FT-IR grade) with a Mattson 7000 FT-IR spectrometer with resolution 8 and 256 interferograms.

The optical spectra were recorded using a Jasco V-560 UV-vis spectrophotometer; all the samples were recorded in the absorbance mode.

Zeta potential measurements were performed using a Zeta Sizer Nano Series (Malvern) instrument. For these measurements, aqueous suspensions of graphene nanocomposites were first submitted to sonication to promote a good dispersion of the graphene sheets.

A Digital Instruments MultiMode scanning probe microscope (SPM) with a Nanoscope IIIA controller in tapping mode was used for the AFM measurements.

FT-Raman spectra were recorded using a Bruker RFS100/S FT-Raman spectrometer (Nd:YAG laser, 1064 nm excitation).

### 3. Results and Discussion

**Characterization of Graphene Substrates.** The chemical exfoliation of graphite in aqueous media resulted in thin sheets of graphene oxide (GO) that readily forms stable colloidal suspensions in water. SEM images revealed the translucent GO sheets with wrinkles and folds (Figure 1).

AFM was used to measure the thickness of the individual GO nanosheets (Figure 2). The average thickness of most GO nanosheets is around 1.8 nm that is larger than the value of 0.8 nm referred for a single-layer graphene.<sup>25,26</sup> Considering that the presence of the oxygen-containing

functional groups on both sides of the GO surfaces increases their thickness with respect to nonfunctionalized graphene sheets,<sup>27</sup> we may consider that most of our GO nanosheets consists of two or three layers of graphene. This result indicates the efficiency of the chemical treatment applied to exfoliate graphite into separate graphene nanosheets.

The presence of the oxygen functionalities at GO surface and the different density of oxygen groups at the different graphene surfaces subjected to thermal and chemical treatments were confirmed by the FTIR spectra. Figure 3 shows the typical FTIR spectrum obtained for the three graphene substrates (GO, GTR and GHR). The characteristic features in the FTIR spectrum of GO are the absorption bands corresponding to the C=O carbonyl stretching vibrations at 1720  $\text{cm}^{-1}$ , the C–OH stretching at 1227  $\text{cm}^{-1}$ , and the C–O stretching at 1070  $\text{cm}^{-1}$ .<sup>28–30</sup> The spectrum also shows a C=C peak at 1620  $\text{cm}^{-1}$  corresponding to the remaining  $\text{sp}^2$  character.<sup>21</sup> In the FTIR spectra of GTR and GHR obtained after thermal and chemical treatment of GO, respectively, only residual presence of bands at  $\sim 1720$ , 1227, and 1070  $\text{cm}^{-1}$  were detected and in the case of the GHR almost no signal of these bands can be detected. Note that all spectra show a band at 1620  $\text{cm}^{-1}$  attributed to aromatic carbon double bonds. Thus, FTIR spectroscopy provided evidence of the presence of different types of oxygen functionalities on the GO material and their decrease in intensity or even suppression after thermal or chemical treatment.

To further study the surface properties of each type of graphene substrate, the zeta potential of aqueous suspensions of GO, GTR and GHR were measured in function of pH (Figure 4). The results achieved show that GO sheets are highly negatively charged  $-35$  mV (average value) at pH range between 3 and 9, which can be attributed to the presence of the above-described oxygen species at the surface of GO. On the contrary, GTR and GHR show zeta potential values near zero for the pH same range, which is indicative of the lower charge density of these type of graphene.

The thermal and chemical treatments of the GO nanosheets resulted, as expected, in the reduction and almost complete elimination (in the case of GHR) of the oxygen functionalities at the surfaces of these materials. These results will be the key for the interpretation of the results presented in the next section.

**Characterization of Graphene/Gold Nanocomposites.** Gold nanoparticles were synthesized from the reduction of a diluted solution of Au(III) complex ions with sodium citrate in the presence of the three types of graphene

(25) Novoselov, K. S.; Geim, A. K.; Morozov, S. V.; Jiang, D.; Zhang, Y.; Dubonos, S. V.; Grigorieva, I. V.; Firsov, A. A. *Science* **2004**, *306*, 666.

(26) Gupta, A.; Chen, G.; Joshi, P.; Tadigadapa, S.; Eklund, P. C. *Nano Lett.* **2006**, *6*, 2667.

(27) Schniepp, H. C.; Li, J. L.; McAllister, M. J.; Sai, H.; Herrera-Alonso, M.; Adamson, D. H.; Prud'homme, R. K.; Car, R.; Saville, D. A.; Aksay, I. A. *J. Phys. Chem. B* **2006**, *110*, 8535.

(28) Stankovich, S.; Piner, R. D.; Nguyen, S. T.; Ruoff, R. S. *Carbon* **2006**, *44*, 3342.

(29) Paredes, J. I.; Villar-Rodil, S.; Martínez-Alonso, A.; Tascon, J. M. D. *Langmuir* **2008**, *24*, 10560.

(30) Bourlino, A. B.; Gournis, D.; Petridis, D.; Szabo, T.; Szeri, A.; Dekany, I. *Langmuir* **2003**, *19*, 6050.



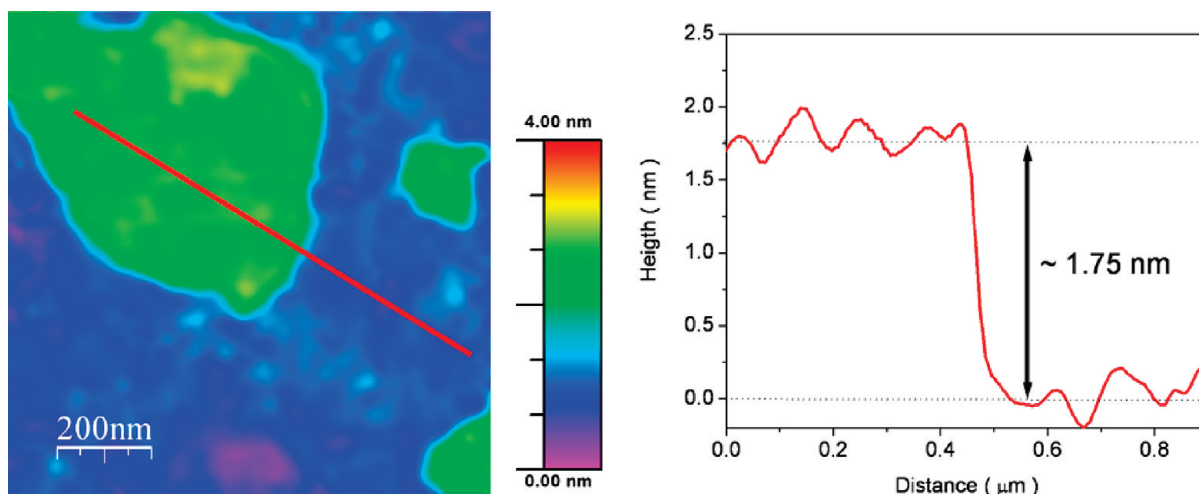


Figure 2. (a) Topographic view of contact-mode AFM scan of GO deposited on SiO<sub>2</sub> glass. (b) Height profile through the line shown in part (a).

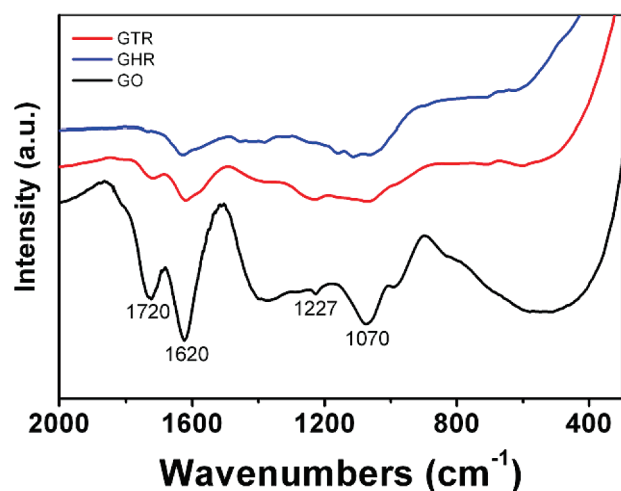


Figure 3. FTIR spectra of the nanocomposites GO, GTR and GHR.

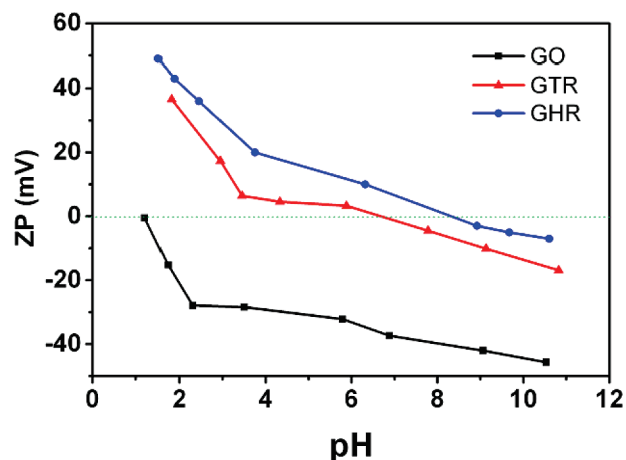


Figure 4. Zeta potential of graphene suspensions GO, GTR and GHR in function of pH.

nanosheets previously described. These substrates were thoroughly washed after the synthesis to remove any gold nanoparticles that were not linked to their surface.

The typical optical spectrum of graphene is characterized by a high reflectance across the visible region and

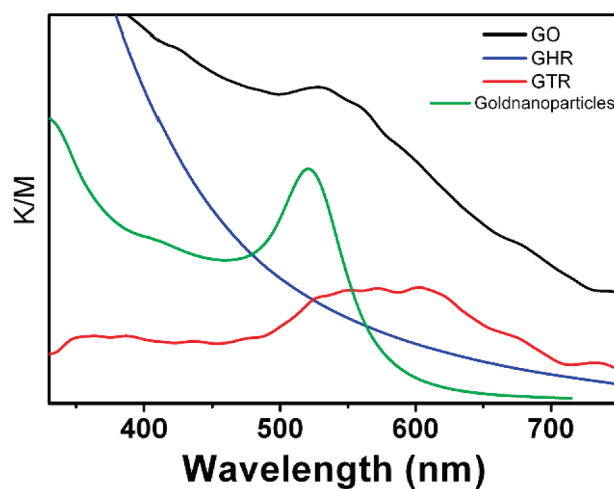
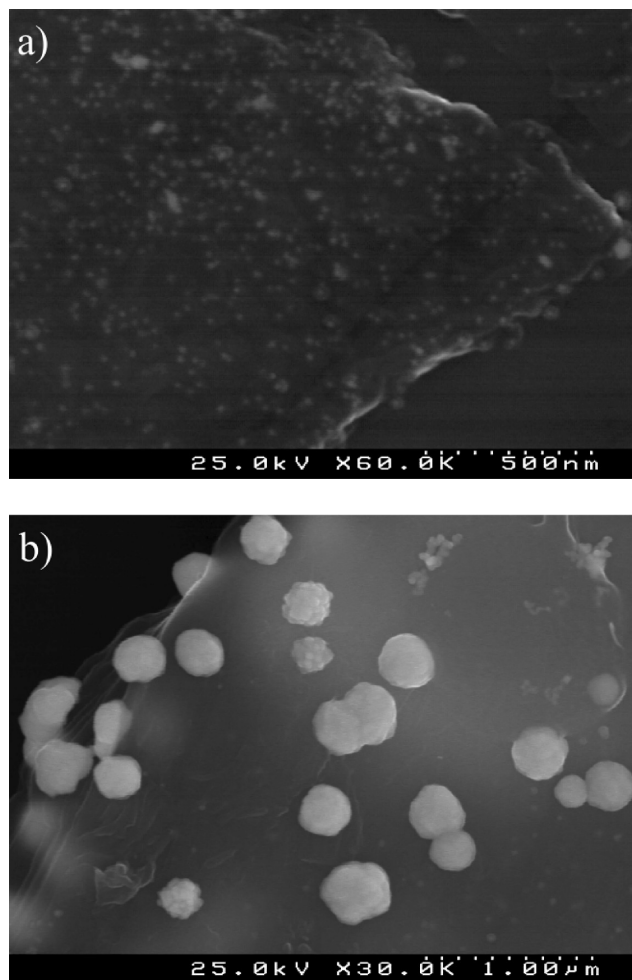


Figure 5. Visible spectra of graphene/Au nanocomposites GO, GTR, and GHR and gold nanoparticles (20 nm).

strong absorption in the ultraviolet region, i.e. for wavelengths lower than 350 nm. For the detection of the gold nanoparticles, the spectra of our materials were recorded in the visible range. Au nanospheres typically show a band around 520 nm in the visible spectrum due to the surface plasmon resonance.<sup>31</sup> Figure 5 shows the visible optical spectra of aqueous suspensions (1.5 mg/mL) of the three different graphene substrates obtained after the synthesis of gold nanoparticles in their presence. For comparison, the spectra of Au colloid prepared using the same methodology in the absence of graphene is shown. As can be observed, there is no evidence of the presence of gold nanoparticles at the surface of GHR in this spectrum range. On the other hand, GO and GTR suspensions show the presence of characteristic absorption bands of gold particles. A rather broad absorption band shift to higher wavelengths is verified for GTR/Au nanocomposite suggesting the presence of particles aggregates. The observed blue tonality of GTR/Au suspension is consistent with the presence of gold particles agglomeration. In the case of the GO/Au aqueous suspension,

(31) Orendorff, C. J.; Sau, T. K.; Murphy, C. J. *Small* **2006**, 2, 636.



**Figure 6.** Scanning electron micrographs of graphene/Au nanocomposites (a) GO and (b) GTR.

the slightly red color observed is in agreement with dispersed gold particles.

Scanning electronic microscopy analysis of these materials confirmed the previous optical results. In fact, at the surface of GHR no gold nanoparticles were observed. On the other hand, a homogeneous distribution of discrete gold nanoparticles with diameters around 20 nm was observed at GO surface (Figure 6a) with negligible nanoparticle agglomeration. At the GTR surfaces, Au nanoparticles agglomerates with diameters of around 300 nm were observed together with a scarce distribution of isolated nanoparticles (Figure 6b).

According to the results presented so far, it is evident that the surface treatment of the graphene sheets has a major role on the nucleation and growth of Au NPs, as the oxygen functionalities are responsible for the gold nanoparticle attachment to the graphene surfaces. As discussed before, on the basis of FTIR and zeta potential measurements, the GO substrate presents a higher density of oxygen functionalities at its surface. The thermal treatment of GO resulted in an exothermic decomposition of hydroxyl and epoxide groups of the GO,<sup>12</sup> although in this case, the treatment at 1050 °C during 30s applied was not enough for the complete reduction of the oxygen groups, as verified in FTIR. From the optical

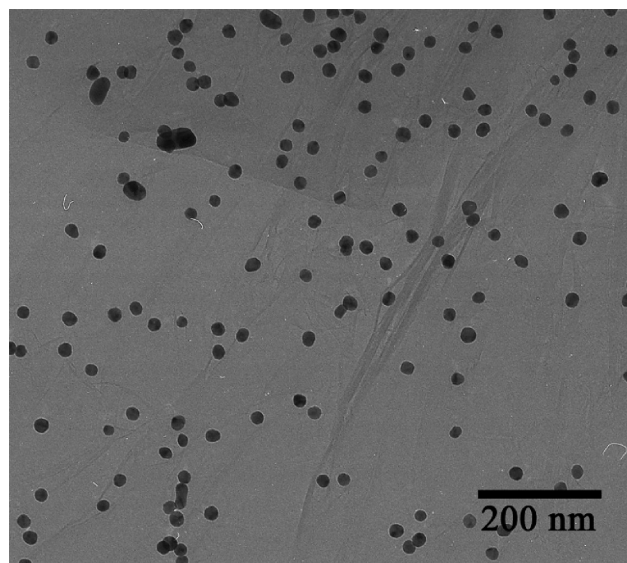


**Figure 7.** Transmission electron micrograph of graphene/gold nanocomposite prepared from GO.

and SEM analysis, it is suggested that a higher density of oxygen functional groups promoted the dispersion of the gold NPs along the graphene surface. On the contrary, a lower density of these groups promoted the growth of gold nanoparticles agglomerates. The absence of Au NPs at GHR demonstrates the importance of the oxygen groups at the graphene surface for the nucleation and growth of Au NPs.

The nanocomposite prepared from GO was further characterized because only this material resembles the real characteristics of a nanomaterial, that is, a multiphase solid material where one of the phases has a dimension of less than 100 nm.<sup>32</sup> The TEM micrograph in Figure 7 depicts a representative image of this nanocomposite. Analysis of the image shows a homogeneous distribution of gold nanoparticles at graphene surface with an average particle size of  $21.3 \pm 1.8$  nm. The thin structure of the graphene sheet and smooth surface are confirmed and some corrugation is detected, suggesting a flexible structure of the graphene sheets.

The dispersion of the gold nanoparticles on the 2D sheet of carbon can be visualized in the AFM image in Figure 8. The AFM analysis further confirms the ability to attain a uniform distribution of 20 nm diameter gold nanoparticles anchored on the graphene nanosheets. The corrugated nature of the graphene sheets is also evident by this analysis.

As discussed previously, the results points out that only GO is suitable for the preparation of gold–graphene nanocomposites under the present experimental conditions. The nucleation of gold nanoparticles at GO surfaces should be mainly governed by the presence of oxygen groups at GO which contribute to an overall negatively charged surface as confirmed by zeta potential measurements. Although it is not possible to make a

(32) Ajayan P. M.; Braun P. V. *Nanocomposite Science and Technology*; Wiley VCH: Weinheim, Germany, 2003.

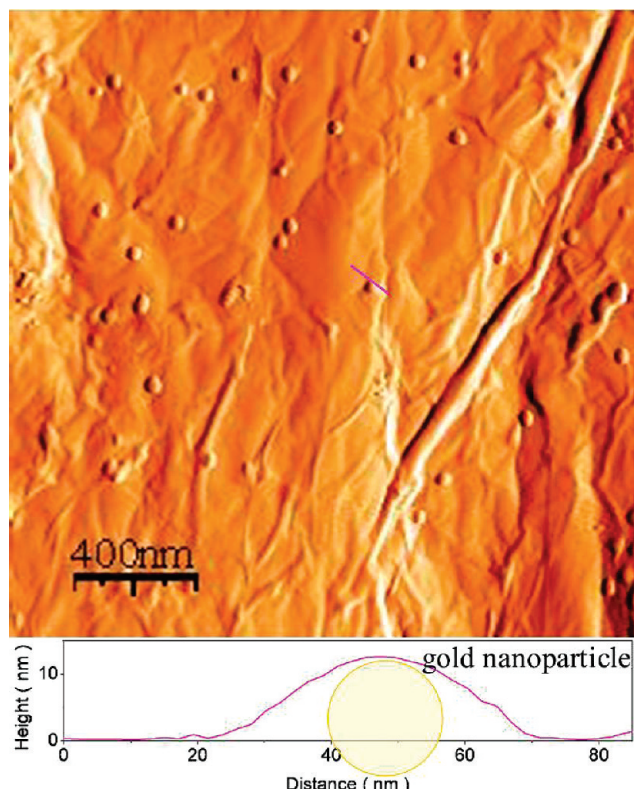


**Figure 8.** AFM image of graphene/gold nanocomposite prepared from GO.

distinction between the roles of each oxygen group (carbonyl, carboxylic, or other) present at GO surface on the nucleation of Au nanoparticles, it is supposed that the overall oxygen functional groups are responsible for a previous attachment of the free gold(III) ions in solution because of electrostatic interactions. The starting experimental reaction step of aging the solution containing gold ions in the presence of graphene has this main propose. Afterward, the addition of the reducing agent (citrate ion) to the precursor solution promotes the subsequent reduction of gold(III) ions, enabling the growth of gold nanoparticles at the graphene surface. The scheme presented in Figure 9 illustrates the reaction steps involved in the above discussion.

**Potential Application for the Prepared Graphene/Gold Nanocomposite As SERS Substrate.** Surface-enhanced Raman scattering (SERS) occurs when molecules are adsorbed on nanostructured surfaces, nanoparticles, or rough electrodes of noble metals and is one of the most powerful microanalytical techniques with single-molecule capabilities and chemical specificity. Recently, SERS has been exploited for biodetection (of protein, DNA, and other biomolecules) by using functionalized gold nanoparticles.<sup>33,34</sup> The SERS effect results from the combination of two main mechanisms designated by electromagnetic and chemical mechanisms. The electromagnetic enhancement involves the excitation of surface plasmons on the metal structures, whereas the chemical

enhancement involves the formation of a charge-transfer complex between the metal and the analyte. Different types of SERS substrates have been developed involving either pure or supported nanostructured metals, mostly gold and silver.<sup>35,36</sup>

In this work, the potential application of the gold-graphene nanocomposite as substrate for SERS was evaluated. SERS was tested for Rhodamine 6G (R6G) using a laser source of 1064 nm. Figure 10 shows the Raman spectrum obtained for R6G adsorbed at the surface of the graphene/gold nanocomposite, together with the one obtained for R6G adsorbed at a single graphene surface (the Raman spectrum of solid R6G is also presented for comparison). The Raman spectrum of R6G adsorbed at a single graphene substrate (Figure 10-Gra) shows only a large broadband in the 1600–1300  $\text{cm}^{-1}$  region, composed by the so-called G and D peaks of graphene.<sup>37</sup>

A good SERS signal was obtained for R6G adsorbed at graphene/gold nanocomposite in contrast with the absence of signal from R6G adsorbed at the single graphene surface. The SERS spectrum (Figure 10-GAu) shows a selective enhancement of bands when compared to the Raman of solid R6G. The SERS signals observed at 1308, 1360, and 1504  $\text{cm}^{-1}$  (Figure 10-GAu) are assigned to the aromatic C–C stretching vibrations of R6G molecule, according to literature reports on the SERS of R6G.<sup>38–40</sup> The SERS spectrum obtained for R6G in the graphene/gold nanocomposite (in the range 1300–1550  $\text{cm}^{-1}$ ) is similar to the R6G SERS spectra found in the literature using different types of gold substrates such as gold nanochains,<sup>38</sup> gold-coated 3D ordered colloidal crystal films,<sup>40</sup> Au-coated ZnO nanorods,<sup>41</sup> or mechanically ruptured nanoporous gold.<sup>42</sup> R6G has been largely used for testing new SERS substrates<sup>38–42</sup> and in detection level studies; the lower detection limit was not evaluated in this work and is under study.

The TEM and AFM images of the graphene/gold nanocomposite (Figures 7 and 8, respectively) show a low density of gold nanoparticles on the graphene substrate, approximately 8.4% (calculated from the area of gold nanoparticles/area of graphene substrate, obtained from the TEM image); it is also clearly observed that there is a high interparticle distance, as the gold NPs are isolated from each other.

Single nanoparticle and single molecule SERS of R6G has been reported using silver substrates.<sup>39,43</sup> For single

(33) Bizzarri, A. R.; Cannistraro, S. *Nanomedicine* **2007**, *3*, 306.

(34) Huang, P.-J.; Chau, L.-K.; Yang, T.-S.; Tay, L.-L.; Lin, T.-T. *Adv. Funct. Mater.* **2009**, *19*, 242.

(35) Banholzer, M. J.; Millstone, J. E.; Qin, L.; Mirkin, C. A. *Chem. Soc. Rev.* **2008**, *37*, 885.

(36) Marques, P.; Nogueira, H. I. S.; Pinto, R. J. B.; Neto, C. P.; Trindade, T. *J. Raman Spectrosc.* **2008**, *39*, 439.

(37) Arsat, R.; Breedon, M.; Shafiei, M.; Spizziri, P. G.; Gilje, S.; Kaner, R. B.; Kalantar-Zadeh, K.; Wlodarski, W. *Chem. Phys. Lett.* **2009**, *467*, 344.

(38) Polavarapu, L.; Xu, Q. H. *Langmuir* **2008**, *24*, 10608.

(39) Pristinski, D.; Tan, S.; Erol, M.; Dul, H.; Sukhishvili, S. *J. Raman Spectrosc.* **2006**, *37*, 762.

(40) Lu, L.; Randjelovic, I.; Capek, R.; Gaponik, N.; Yang, J.; Zhang, H.; Eychmüller, A. *Chem. Mater.* **2005**, *17*, 5731.

(41) Sakano, T.; Tanaka, Y.; Nishimura, R.; Nedyalkov, N. N.; Atanasov, P. A.; Saiki, T.; Obara, M. *J. Phys. D: Appl. Phys.* **2008**, *41*, 235304.

(42) Qian, L. H.; Inoue, A.; Chena, M. W. *Appl. Phys. Lett.* **2008**, *92*, 093113.

(43) Nie, S. M.; Emery, S. R. *Science* **1997**, *275*, 1102.





Figure 9. Schematic representation of the mechanism of nucleation of gold nanoparticles at functionalized graphene surface.

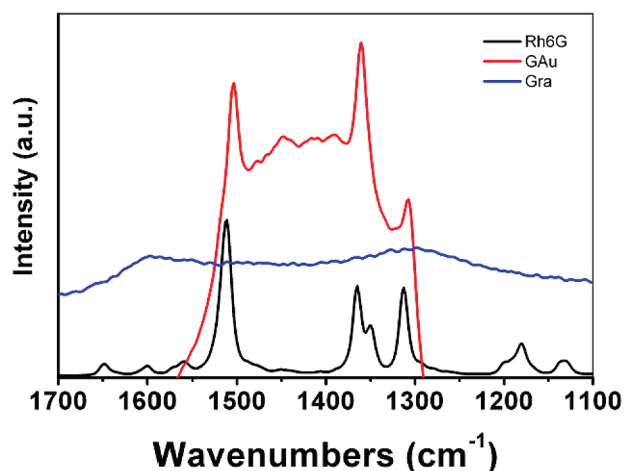


Figure 10. SERS spectrum of Rh6G adsorbed at the surface of graphene/gold nanocomposite (GAu) and Raman spectra of R6G adsorbed at a single graphene sheet (Gra) and of solid Rh6G (Rh6G).

R6G molecules adsorbed on the selected nanoparticles, the intrinsic Raman enhancement factors reported were on the order of  $1 \times 10^{14}$  to  $1 \times 10^{15}$ , much larger than the ensemble-averaged values derived from conventional measurements.<sup>43</sup> The above TEM and AFM observed characteristics of the graphene/gold nanocomposite prepared in this work, in particular the interparticle distance and particle isolation on the graphene surface, lead us to induce that the observed R6G SERS signal may possibly originate from single gold nanoparticle SERS mechanisms.<sup>44</sup> We can also consider that the combination of gold

nanoparticles and graphene may confer a unique electron or energy transfer mechanism between both phases that allows the SERS observation.

The SERS observation provided evidence for the surface binding of R6G and demonstrated that the graphene–nanoparticle combination functions as SERS substrate. This graphene/gold nanocomposite substrate may present advantages for instance on single gold nanoparticle SERS studies.<sup>44</sup>

#### 4. Conclusions

Here, we show that the presence of oxygen functionalities at graphene surface provides reactive sites for the nucleation and growth of gold nanoparticles. Gold nanoparticles are effectively grown at functionalized graphene surfaces using a simple chemical method in aqueous medium. The nucleation and growth mechanism depends on the degree of oxygen functionalization at the graphene surface sheets, no gold nanoparticles are obtained at totally reduced graphene surfaces. Additionally, our studies indicate that the graphene/gold nanocomposites may function as substrates for surface enhanced Raman scattering. These findings are expected to provide new design parameters of novel nanostructures for potential applications such as biosensors, controlled drug delivery, and spectroscopic probes.

**Acknowledgment.** G.G. thanks the INL (International Iberian nanotechnology laboratory) for the financial support of this work. Thanks are also due to Fundação para a Ciência e a Tecnologia (Portugal) for a post graduation grant to C.M.G. (SFRH/BD/30137/2006).

(44) Talley, C. E.; Jackson, J. B.; Oubre, C.; Grady, N. K.; Hollars, C. W.; Lane, S. M.; Huser, T. R.; Nordlander, P.; Halas, N. J. *Nano Lett.* **2005**, *5*, 1569–1574.